

Original Article

VEGF-C mediated enhancement of lymphatic drainage reduces intestinal inflammation by regulating IL-9/IL-17 balance and improving gut microbiota in experimental chronic colitis

Xiaolei Wang¹, Jin Zhao², Li Qin²

¹Department of Gastroenterology, Shanghai Tenth People's Hospital, Tongji University, Shanghai 200072, China;
²Department of Gastroenterology, Shanghai Tongji Hospital, Tongji University, Shanghai 200065, China

Received September 4, 2017; Accepted October 16, 2017; Epub November 15, 2017; Published November 30, 2017

Abstract: Background: Inflammation-associated lymphangiogenesis (IAL) induced by vascular endothelial growth factor (VEGF)-C/VEGF receptor-3 (VEGFR-3) pathway plays a crucial role in chronic intestinal inflammation. This study aimed to investigate the effects of VEGF-C mediated enhancement of lymphatic drainage on the intestinal inflammation in experimental chronic colitis (CC) and the potential mechanism was explored. Methods: Mouse CC model was established by three cycles of 2% DSS administration for 5 days following water administration for 5 days. CC mice were injected via the tail vein with AD-VEGF-C-EGFP (VEGF-C+DSS group) or AD-EGFP (AD-EGFP group) at the end of each cycle and animals in control group were given access to drinking water only. Disease activity index (DAI), lymphatic vessel density (LVD), colonic cytokines, Th9 cells (CD3⁺ cells) and CD68⁺ macrophage infiltration, and lymph flow were detected. Fresh feces were collected and processed for DNA extraction and MiSeq Illumina sequencing of V4 region of bacterial 16S rRNA gene. Alpha- and beta diversities and compositional differences at phylum and genus levels were determined in intestinal microbiota. Results: AD-VEGF-C treatment significantly reduced colon inflammation, elevated the increase in lymph drainage, decreased CD68⁺ macrophages and CD3⁺ T cells (Th9 cells), reduced IL-9, and increased IL-17 in colon mucosa when compared with DSS mice. In addition, VEGF-C treated mice showed significantly increased the abundance of Bacteroidate and decreased Firmicutes at phylum level in fecal samples. Conclusion: VEGF-C improves intestinal inflammation by enhancing lymphatic drainage, reducing intestinal Th9 cells, regulating intestinal IL-9/IL-17 balance and increasing intestinal Bacteroidate abundance in CC mice.

Keywords: Lymphatic drainage, intestinal microbiota, vascular endothelial growth factor C, Th9 cells, interleukin-9, chronic colitis

Introduction

Inflammatory bowel diseases (IBD) are chronic, inflammatory disorders of the gastrointestinal tract and a deregulation of the T cell-mediated immune response toward the intestinal bacteria plays an important role in the pathogenesis of IBD [1]. The inflammatory response to pathogens in IBD is characterized by the bacterially driven, aberrant immune-mediated response in genetically susceptible hosts. The efficient lymphatic drainage is required to reduce those harmful agents in the hostile microenvironment, such as microbes, increased cytokines in

blood and tissues, and the excessive interstitial fluid and edema.

Lymphatic vessels are crucial for the regulation of tissue fluid clearance and immune cells recruitment. Accumulating evidence indicates that inflammation-associated lymphangiogenesis (IAL) may influence the mucosal edema and/or leukocyte infiltration. Among many prolymphangiogenic signaling pathways, the VEGF-C/VEGFR-3 is the best characterized in the process of IAL and has been widely studied. Mice treated with anti-VEGFR-3 antibody exhibited a significant increase in the number of enlarged

lymphatic vessels in the colon submucosa, accompanied by a significant decrease in the severity of inflammation compared to control mice [2]. Systemic delivery of VEGF-C to simulate lymphatic drainage and enhance lymphangiogenesis markedly reduces chronic intestinal inflammation [3]. However, whether lymphatic drainage and/or lymphangiogenesis affect the compositional (dysbiosis) shifts of intestinal microbiota in relation to VEGF-C treatment and improve inflammation in mice with chronic colitis (CC) is unknown.

Immune cells and cytokines are involved in the pathogenesis of IBD. Th9 cells, a novel subset of Th cells that primarily produces interleukin (IL)-9, have recently been found to be associated with the development of inflammatory diseases [4]. Experimental models of colitis highlight that IL-9-producing T cells critically interfere with the barrier function of the intestinal epithelium [5], and IL-9 deficiency suppresses acute and chronic colitis [6]. Whether enhancing lymphatic drainage can affect the number of Th9 cells and colonic IL-9 level, and then further alleviate intestinal inflammation is still unclear. IL-17 is another cytokine which may protect against extracellular bacterial and fungal infections and plays important roles in chronic inflammatory diseases. IL-17 can be produced by innate immune cells in peripheral tissues (such as intestinal mucosa and lungs) of humans and mice [6]. Studies have revealed that IL-17-expressing mast cells promote the proliferation of myeloid-derived suppressor cell (MDSC) [7] to suppress immune responses [8, 9]. However, IL-17 has dual roles in inflammatory diseases. IL-17 deficiency leads to reduced control of infections, but IL-17 overproduction can cause several chronic inflammatory diseases [10]. The contribution of IL-17 remains unclear in IBD. In this study, VEGF-C was employed to enhance lymphatic drainage, then the colon inflammation, gut microbiota, immune cells and cytokines were investigated, and the association between IL-9/IL-17 cytokines balance and intestinal inflammation was further evaluated.

Materials and methods

Mice

This study has been approved by the Ethics Committee of Shanghai Tenth People's Hos-

pital. And we have observed the Interdisciplinary Principles and Guidelines for the Use of Animals in Research, Testing, and Education by the New York Academy of Sciences, Ad Hoc Animal Research Committee. CC model was induced in mice by administration of dextran sodium sulfate (DSS), A total of 34 female C57BL/6 mice aged 8-12 weeks were purchased from the Shanghai Laboratory Animal Center (Shanghai, China). Animals were housed under a specific pathogen-free (SPF) condition in the Experimental Animal Center of Tongji Hospital. Mice were given *ad libitum* access to food and water. All animal experiments were conducted in accordance with the Guidelines for the Care and Use of Laboratory Animals of Tongji University.

Construction and expression of recombinant adenoviruses encoding VEGF-C

The adenovirus vector pAd-VEGF-C-IRES-EGFP was constructed by cloning the gene encoding human VEGF-C (GenBank accession NM_005429.2) under the cytomegalovirus promoter in the pAd/CMV/V5-DEST vector. Human embryonic kidney 293 cells were used to produce replication-deficient recombinant adenovirus, which was then concentrated. The titer of recombinant adenovirus (Ad-VEGF-C-EGFP) obtained was 1.75×10^{11} plaque-forming units (PFU)/mL. Empty vector AD-EGFP was used as the control and amplified to a titer of 1×10^{10} PFU/mL. Real time quantitative-PCR was used to determine the expression of AD-VEGF-C-EGFP *in vitro*. The primers for VEGF-C were 5'-GTGCATGAACACCAGCAGAG-3' (forward) and 5'-TCCAGCATCCGAGGAAAACA-3' (reverse). The relative mRNA expression of VEGF-C was normalized to that of human GAPDH which was measured with following primers: 5'-GGGTGTGAACCATGAGAAGTATG-3' (forward) and 5'-GATGGCATGGACTGTGGTCAT-3' (reverse).

DSS-induced CC and grouping

CC was induced by drinking 2% DSS (MW 36,000-50,000; MP Biomedical) *ad libitum* for 5 days, and then mice drunk DSS free water for another 5 days for 3 cycles (**Figure 1**). DSS water was freshly prepared every day. Mice were grouped according to their body weight. Mice in VEGF-C group (n=12) were injected via the tail vein with 100 μ l of AD-VEGF-C-EGFP ($5 \times 10^{8-9}$ PFU) at the end of each cycle, while

VEGF-C mediated lymphatic drainage enhancement reduces intestinal inflammation

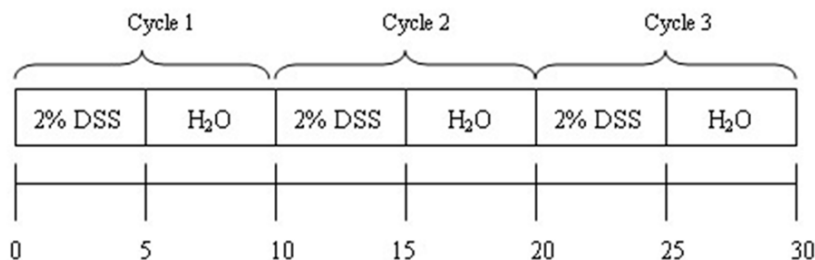


Figure 1. Schematic chart of study design.

mice in DSS group (n=12) were injected with AD-EGFP. Control mice (n=10) drunk normal water only. Mouse body weight, stool consistency/diarrhea, and rectal bleeding (Hemocult test kit, Nanjing Jiancheng Technology Co., Ltd., China) were recorded once daily to determine the disease activity index (DAI) according to previously reported [11, 12]. Scores were defined as: W) weight loss: 0 (0-1%), 1 (1-5%), 2 (5-10%), 3 (10-20%), and 4 (>20%); S) stool consistency: 0 (normal), 2 (loose stools), and 4 (diarrhea); B) hemafecia: 0 (no blood), 1 (hemocult positive), 2 (hemocult positive and visual pellet bleeding), and 4 (gross bleeding, blood around anus). The final macroscopic score was the sum of each individual score. Mice were euthanized by CO₂ inhalation, followed by cervical dislocation on day 38. The entire colon length was measured from the end of the cecum to the anus. Then, a 1.5-cm distant colon was collected, fixed in 10% formalin and embedded in paraffin for histological examination.

Histological examination of the colon

Each colon sample was divided into three parts (proximal, middle and distal), and fixed in 10% buffered formalin solution. Paraffin-embedded sections (5 μ m in thickness) were subjected to hematoxylin/eosin (H&E) staining. The sections were graded as to crypt score, hyperplastic epithelium, crypt distortion (distorted epithelium), and inflammation (acute and chronic). The score was evaluated according to previously reported and calculated by the product of grade multiplied by the extent of involvement [11]. Crypt distortion and hyperplastic epithelium were graded according to their extent of involvement (as per crypt scores and inflammation) for each sample, the scores summed, and divided by the numbers of pieces of tissue for each seg-

ment. Histological examination was independently performed by two pathologists blind to the study [11].

Immunohistochemistry (IHC) and immunofluorescence staining

For histochemical staining, paraffin-embedded sections of the distant colon were obtained (5-mm thickness) from each sample. The lymphatic vessels (LYVE-1-positive structures with lumina) were detected by immunohistochemistry for LYVE-1 (ab14917, 1:200, Abcam), and the percentage of colon tissue with large and tortuous lymphatic vessels was calculated. In brief, vessels positive for LYVE-1 were inspected by light microscopy at 10 \times magnification. Five areas of tissue with the highest density of lymphatic vessels were selected ("hot areas"). Lymphatic vessel density (LVD) was assessed by counting all stained vessels in these regions and the mean number of the total counted vessels determined as LVD (per mm³). Computer-assisted analyses of digital images were performed using the NIS Elements 4.0 Microscope Imaging Software (Nikon) as described previously [3]. Morphometric analyses were performed using the Photoshop Extended CS4 software (Adobe Systems Inc., San Jose, CA). The area covered by lymphatic vessels (lymphatic vessel density) and lymphatic vessel size were measured. The average size of vessels per area was calculated (per μ m³). The counting of vessels were performed independently by two investigators blind to this study.

In brief, sections were treated with 0.3% H₂O₂ for 10 min at room temperature, followed by antigen retrieval in 0.01 mmol/L sodium citrate (pH 6.0). Slides were incubated at 4°C overnight with primary antibodies (anti-mouse LYVE-1 polyclonal antibody, anti-mouse CD3 antibody [1:100; ab5690, Abcam, Cambridge, UK]; anti-mouse CD68 [1:200; BD Pharmingen]) for the detection of Th9 cells and macrophages. Sections were rinsed thrice in 0.1 mmol/L PBS for 2 min, and incubated for 30 min at room temperature with goat anti-rabbit/mouse horseradish peroxidase (Envision, DAKO, CA).

VEGF-C mediated lymphatic drainage enhancement reduces intestinal inflammation

DAPI was used to stain nucleus (blue), and FITC to stain LYVE-1 positive vessels (green). Visualization was done with 3' 3-diaminobenzidine. Normal IgG served as a negative control.

Lymphatic drainage assessment [13, 14]

Ten micrograms of Evan blue dye (Sigma Aldrich) in 10 μ l of PBS was injected into the rectal mucosa of anesthetized mice (n=5 per time point) using a Hamilton syringe. After 16 h, mice were killed. Evans blue dye was extracted from the distal colon tissues followed by incubation at 55°C overnight in formamide (Sigma-Aldrich). The absorbance was measured with M200 microplate reader at the wavelength ranging from 620 nm to 740 nm. The concentration of Evan blue dye was calculated from a standard curve.

Enzyme-linked immunosorbent assay (ELISA)

Colon tissues (n=5 per group) were homogenized in lysis buffer containing a protease inhibitor cocktail for radioimmunoprecipitation assay (150 mM NaCl, 50 mM Tris, pH 7.5, Sigma Chemicals). Homogenates were centrifuged for 10 min at 14000 g, and the supernatant was collected for the detection of IL-1 β , IL-6, IFN- γ , IL-4, IL-10, IL-9 and IL-17 with commercially available ELISA kits (ELISA-Quantikine® Colorimetric Sandwich ELISAs, R&D Systems, Minneapolis, Minnesota, United States) according to the manufacturer's instructions. The absorbance was measured with M200 microplate reader (Tecan Group Ltd., Männedorf, Switzerland).

Microbial diversity analysis

DNA extraction and PCR amplification: The fresh feces collected in sterile tubes were frozen at -80°C for analysis of microbiota. In brief, approximately 200 mg of each fecal sample was processed for DNA extraction using the E.Z.N.A.® Soil DNA Kit (Omega Bio-tek, Norcross, GA, U.S.). DNA solution was diluted to 10 ng/ml. The V4 region of bacterial 16S ribosomal RNA gene was amplified by PCR (95°C for 5 min, followed by 27 cycles at 95°C for 30 s, 55°C for 30 s, and 72°C for 45 s and a final extension at 72°C for 10 min) using primers 515F 5'-GTGCCAGCMGCC GCGG-3' and 907R 5'-CCGTC AATTCMTTTRAGTTT-3', where barcode is an eight-base sequence unique to each

sample. PCR was performed in triplicate with 20- μ L mixture containing 4 μ L of 5 \times FastPfu Buffer, 2 μ L of 2.5 mM dNTPs, 0.8 μ L of each primer (5 μ M), 0.4 μ L of FastPfu Polymerase, and 10 ng of template DNA.

Illumina MiSeq sequencing: Amplicons were extracted from 2% agarose gels, purified using the AxyPrep DNA Gel Extraction Kit (Axygen Biosciences, Union City, CA, U.S.) according to the manufacturer's instructions and quantified using QuantiFluor™ -ST (Promega, U.S.). The pooled DNA product was used to construct Illumina Pair-End library following the Illumina's genomic DNA library preparation procedure. Then the amplicon library was paired-end sequenced (2 \times 250) on an Illumina MiSeq platform (Shanghai BIOZERON Co., Ltd.) according to the standard protocols. Data from sequencing were uploaded into the Sequence Read Archive (SRA) of NCBI (<http://www.ncbi.nlm.nih.gov/sra>) (Accession Number: SRP09-5973).

Processing of data from sequencing: Raw fastq files were demultiplexed and quality-filtered using QIIME (version 1.17) with following criteria: (i) The 250 bp reads were truncated at any site receiving an average quality score <20 over a 10-bp sliding window, and the truncated reads that were shorter than 50bp were not used. (ii) Exact barcode matching and 2 nucleotide mismatch in primer matching were allowed. Reads containing ambiguous characters were removed. (iii) Only sequences that overlap longer than 10 bp were assembled according to their overlapping sequence. Reads which could not be assembled were not used. Operational Units were clustered with 97% similarity cutoff using UPARSE (version 7.1 <http://drive5.com/uparse/>), and chimeric sequences were identified and removed using UCHIME. The phylogenetic affiliation of each 16S rRNA gene sequence was analyzed by RDP Classifier (<http://rdp.cme.msu.edu/>) against the silva (SSU123) 16S rRNA database using confidence threshold of 70% [15].

Alpha- and Beta-diversity analyses: Within community diversity (α -diversity) was calculated by different indices of species richness and evenness such as Chao, Sobs and Shannon diversity indices. An even depth of 21,000 and 14,500 sequences per fecal sample was used for the calculation of diversity indices. The

VEGF-C mediated lymphatic drainage enhancement reduces intestinal inflammation

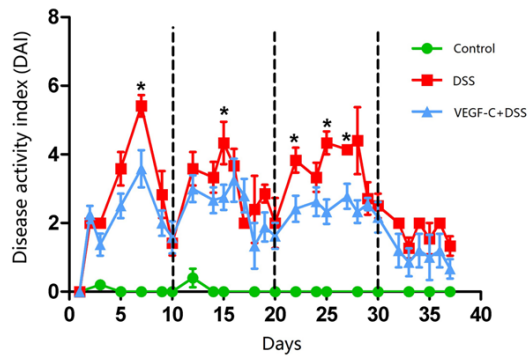


Figure 2. Ad-VEGF-C alleviates colon inflammation (lower DAI scores) in mice with DSS-induced CC as compared to DSS group on days 7, 15, 22, 25 and 27. (* $P < 0.001$).

rarefaction curve was delineated to reveal the diversity using QIIME. Beta-diversity analysis was performed using UniFrac [16] to compare the results of principal component analysis, using the community ecology package, R-forge (Vegan 2.0 package was used to generate a PCA figure). Principal coordinate analysis (PCoA) was applied on resulting distance matrices to generate two dimensional plots using the open source R software (v. 3.1.0) and the P values were calculated using PERMANOVA analyses of Bray-Curtis distances. Differences in alpha-diversity among VEGF-C group, DSS group and control group were determined using SPSS v. 20 (IBM, Armonk, NY, USA). The statistical analysis, LEfSe [17], was used to identify the significant difference in gut microbiota between VEGF-C group and DSS group.

Statistical analysis

All data are expressed as mean \pm standard deviation (SD). For quantitative data, one-way analysis of variances followed by Tukey's test was employed for comparisons. Qualitative data were analyzed by Kruskal-Wallis test followed by selected mean comparisons with Bonferroni correction. For pyrosequencing data, the unweighted Unifrac distance was analyzed by Analysis of Similarities (ANOSIM) in R's vegan package version 2.0-3 implemented into QIIME. Phylum level percentage was compared among VEGF-C group, DSS group and control group by Wilcoxon rank-sum test using SPSS version 20 (IBM, Armonk, NY, USA). The comparisons of DAI, macroscopic scores, weight loss score and inflammatory markers were performed using

one-way ANOVA followed by Tukey-Kramer post hoc analysis, using prism (Prism 5, GraphPad, La jolla, CA, USA). A value of $P < 0.05$ was considered statistically significant.

Results

VEGF-C alleviated DAI and histological score in CC mice

Mice treated with 2% DSS were Hemocult positive on day 3, and displayed more severe bloody diarrhea on day 5. As shown in **Figure 2**, the DAI significantly reduced in AD-VEGF-C treated mice compared with in DSS mice ($P < 0.05$, 2.00 ± 0.16 vs 2.74 ± 0.23), especially on days 7, 15, 22, 25 and 27 ($P = 0.01$, 0.04 , 0.01 , 0.00 , and 0.01 , respectively).

Mice in DSS group showed more severe histological damage (damage to crypt architecture, cellular infiltration, goblet cell depletion, and submucosal edema) compared with normal mice (**Figure 3A-C**). However, mice in AD-VEGF-C group showed attenuated histological damage compared with mice in DSS group (**Figure 3D**, $P = 0.023$, 4.78 ± 0.44 vs 6.32 ± 0.25). There were mild loss of crypt structure and eroded epithelium in the colon of AD-VEGF-C treated mice compared to mice in DSS group.

VEGF-C treatment modulated lymphatic vessels and lymphatic drainage

In **Figure 4**, the lymphatic vessels after VEGF-C treatment were enlarged and tortuous, and mainly located in the mucosa and lamina propria. There was no significant difference in LVD between AD-VEGF-C group and DSS group (A-D, 19.22 ± 0.80 to 17.34 ± 0.97 , $P > 0.05$). However, the AD-VEGF-C-treated mice had significantly larger lymphatic vessels and increased LVD as compared to mice in DSS group (E, 19.22 ± 0.80 to 17.34 ± 0.97 , 198.0 ± 11.22 to 163.4 ± 7.67 , $P = 0.038$).

To investigate the effect of VEGF-C on lymphatic drainage in CC, Evans blue dye was injected and detected in the distant colonic mucosa. Results revealed that lymphatic drainage increased in AD-VEGF-C treated mice as compared to mice in DSS group (**Figure 5**, 1.85 ± 0.50 vs 1.34 ± 0.17 , $P = 0.042$).

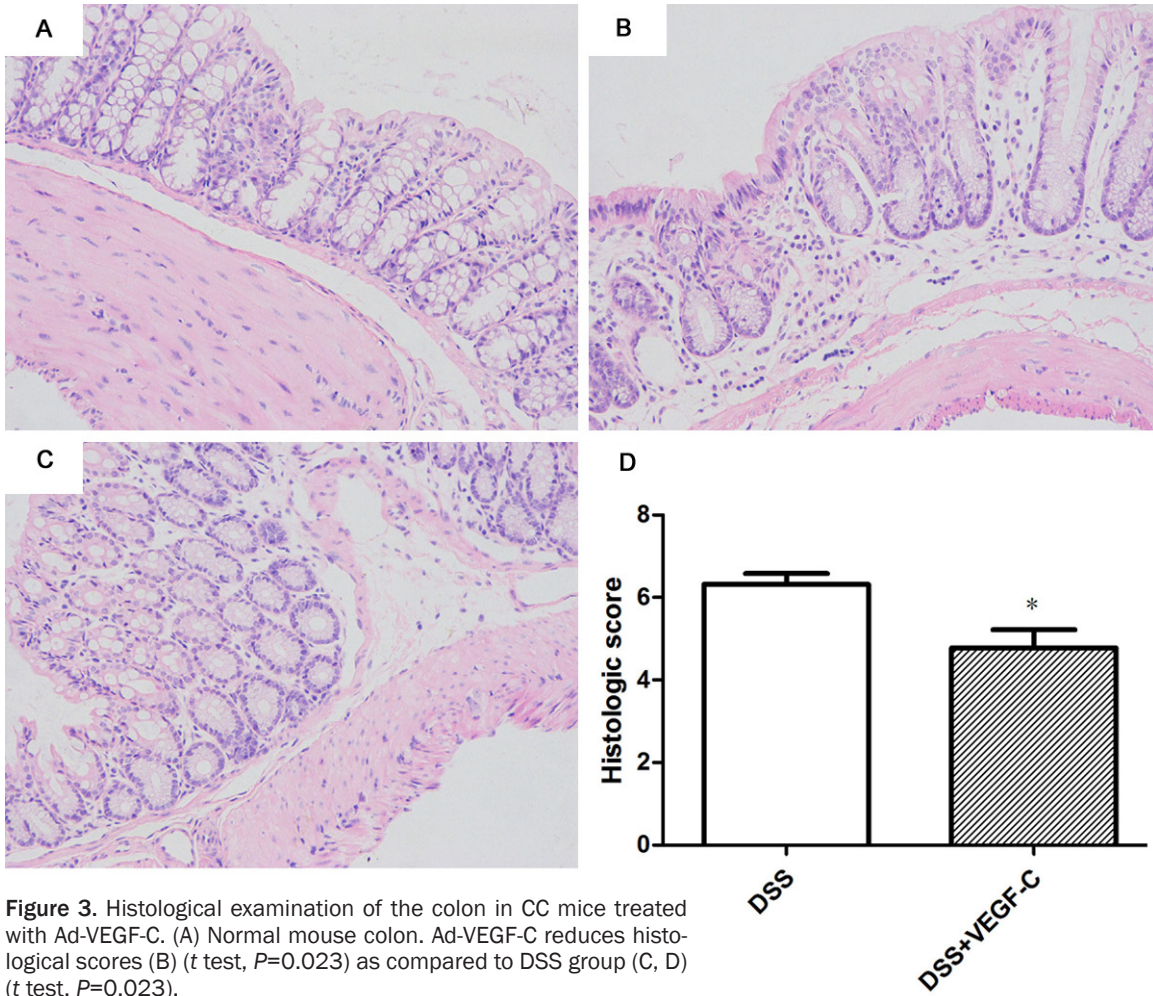


Figure 3. Histological examination of the colon in CC mice treated with Ad-VEGF-C. (A) Normal mouse colon. Ad-VEGF-C reduces histological scores (B) (t test, $P=0.023$) as compared to DSS group (C, D) (t test, $P=0.023$).

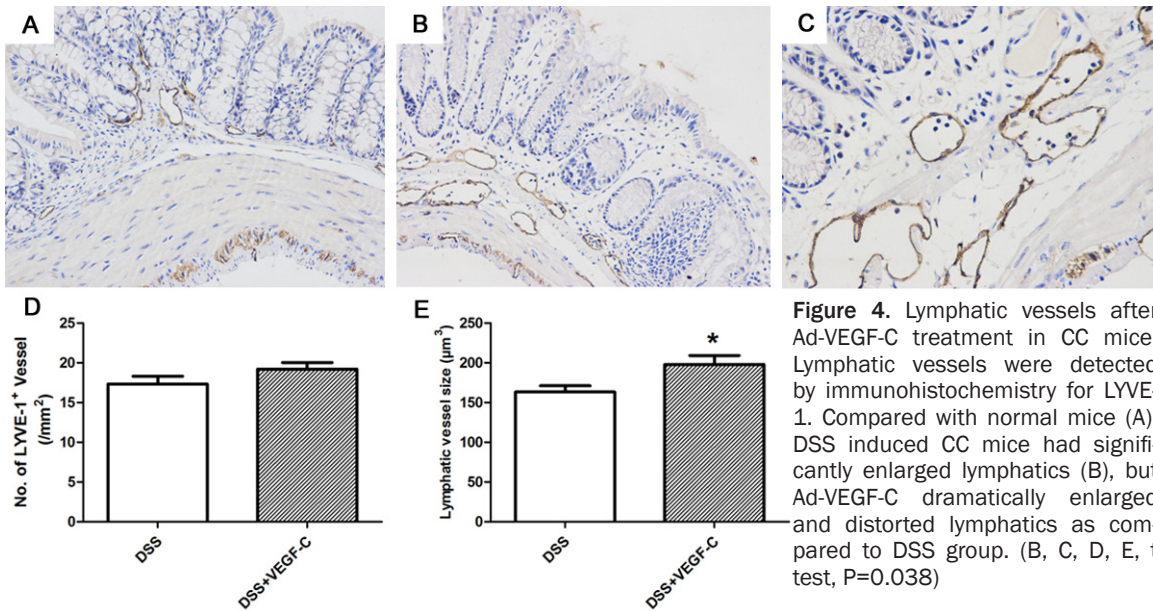


Figure 4. Lymphatic vessels after Ad-VEGF-C treatment in CC mice. Lymphatic vessels were detected by immunohistochemistry for LYVE-1. Compared with normal mice (A), DSS induced CC mice had significantly enlarged lymphatics (B), but Ad-VEGF-C dramatically enlarged and distorted lymphatics as compared to DSS group. (B, C, D, E, t test, $P=0.038$)

VEGF-C mediated lymphatic drainage enhancement reduces intestinal inflammation

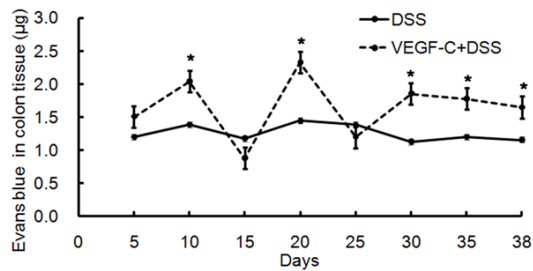


Figure 5. Lymph flow increases in the colon after Ad-VEGF-C treatment in CC. Ad-VEGF-C treated mice had increased lymph flow as compared to mice in DSS group. ($P=0.042$).

Colon cytokines in CC mice after Ad-VEGF-C treatment

Some cytokines in the colon were measured by ELISA. In CC mice, the contents of TNF- α , IL-1 β , IL-4, IL-6, IL-17 and IFN- γ were comparable between AD-VEGF-C group and DSS group (**Figure 6**, $P>0.05$). However, the contents of IL-10 and IL-17 in the colon increased significantly (**Figure 6**, $P=0.0488$, 0.0486 , respectively), and IL-9 markedly reduced in AD-VEGF-C group as compared to DSS group (**Figure 6**, $P=0.035$). These indicate that no immune reaction of innate immune response (TNF- α , IFN- γ , IL-1 β , IL-6), however, mixed reaction of Th9 and Th17 cells.

VEGF-C alters intestinal microflora

The fecal microbiota was further investigated in CC mice after AD-VEGF-C treatment. A total 109,932 valid reads were obtained from 11 samples by MiSeq sequencing ($n=3$ for control group, $n=4$ for DSS group, and $n=4$ for AD-VEGF-C group). The within-sample diversity was calculated using the Shannon index, and the community richness using Chan and Sobs index (**Figure 7A-C**). Results showed that the community richness in AD-VEGF-C group significantly decreased as compared to DSS group ($P<0.05$), however, no significant difference was found in Shannon index ($P>0.05$). These indicate that increased lymphatic drainage in CC mice results in a decreased microflora community richness, but has no influence on the community diversity.

The cluster analysis showed fecal samples grouped tightly. The samples clustered together in the DSS group could be separated from

AD-VEGF-C group. The location of AD-VEGF-C group was closer to healthy controls as compared to DSS group. PCoA indicated significantly difference in the bacterial community between AD-VEGF-C group and DSS group (**Figure 7D**). The rarefaction curves indicated that the sequencing was deep enough to capture most of the operational Units within our samples (**Figure 7E**).

We further investigated the microbiota composition in different groups. At the phylum level, the fecal microbiota was dominated by species of the phyla Bacteroidetes and Firmicutes. The proportion of Bacteroidetes significantly increased after VEGF-C treatment with a relative abundance of 85.62%, when compared with that in DSS group (60.17%) (**Figure 8A, 8B**, $P=0.049$). Meanwhile, the proportion of Firmicutes significant decreased (17.5%) in AD-VEGF-C group as compared to DSS group (30.63%) ($P=0.044$). Moreover, the Bacteroidetes/Firmicutes ratio of the gut microbiota increased from 4.89 in AD-VEGF-C group to 1.96 in DSS group. At the genus level, the bacterial taxa were comparable between AD-VEGF-C group and DSS group (**Figure 8C, 8D**, $P>0.05$). These gut microbiota after AD-VEGF-C treatment in CC mice were improved and close to a healthy profile.

Linear discriminate analysis (LDA) effect size (LEfSe) is a statistical tool designed to find biomarkers from metagenome data with default parameters to identify potential discriminating taxa between two groups. LDA score of 2.5 was used for identifying bacterial groups with statistical significance. Thirty-one taxa with significant difference were found in DSS group, and four taxa showed significant abundance in AD-VEGF-C group (**Figure 9A, 9B**). The clade graph showed that the percentage of All-oprevotella was higher at the genus level, and the gut metagenome, Bacteroides chinchilla and uncultured Erysipelotrichales_bacterium had higher abundance at the species level. Uncultured Erysipelotrichales bacterium belongs to Firmicutes genus, but the other three species belong to Bacteroidetes genus (**Figure 9A, 9B**).

Results from LEfSe showed that there were 35 taxa that could distinguish one group from another with the LDA score greater than 2. One genus and three species showed significantly

VEGF-C mediated lymphatic drainage enhancement reduces intestinal inflammation

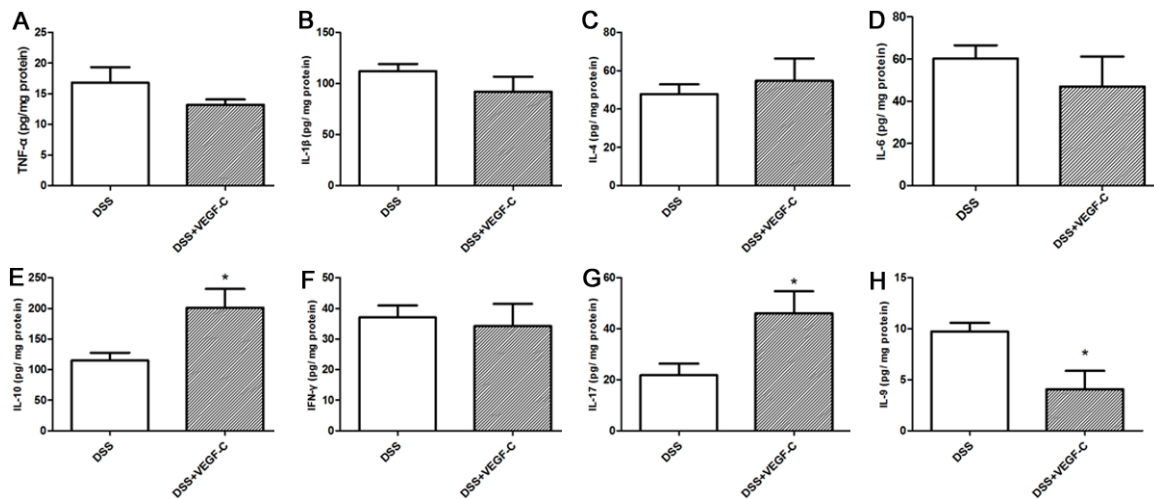


Figure 6. Cytokines increase in the colon after Ad-VEGF-C treatment in DSS-induced CC mice. IL-10 and IL-17 increased significantly and IL-9 markedly reduced in mice treated with Ad-VEGF-C as compared to mice in DSS group (t test, $P < 0.05$). TNF- α , IL-1 β , IL-4, IL-6, and IFN- γ remained unchanged after Ad-VEGF-C treatment ($P > 0.05$).

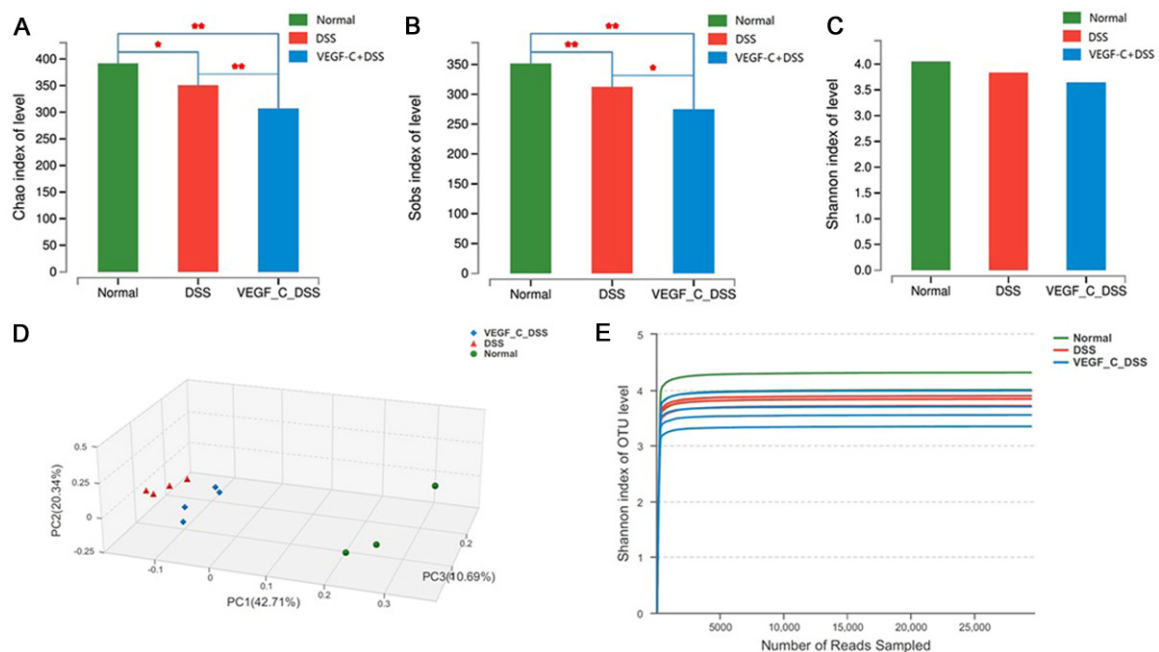


Figure 7. Induction of dysbiosis in C57BL mice after VEGF-C treatment. Both Chao and Sobs index in VEGF-C treated mice markedly decreased as compared to DSS group (A, B). Shannon index was comparable between the groups (C). PCoA indicates samples in VEGF-C group (blue) clustered together and could be differentiated from those in DSS group (red) (D). Rarefaction curves tended to reach the plateau (E).

higher abundance in AD-VEGF-C group. In AD-VEGF-C group, the abundances of *Alloprevotella* genus ($P=0.02092$), *Bacteroides_chinchilla* specie ($P=0.0433$), and *gut_metagenome* specie ($P=0.0209$) from *Bacteroidetes.c* genus increased significantly as compared to DSS group.

VEGF-C decreased colon macrophages and CD4⁺ T cells in CC mice

Colon macrophages and CD4⁺ T cells were detected in CC mice by immunofluorescent staining. Results showed CD68⁺ macrophages (Figure 10A-C, $P=0.038$) and CD3⁺CD4⁺ T cells

VEGF-C mediated lymphatic drainage enhancement reduces intestinal inflammation

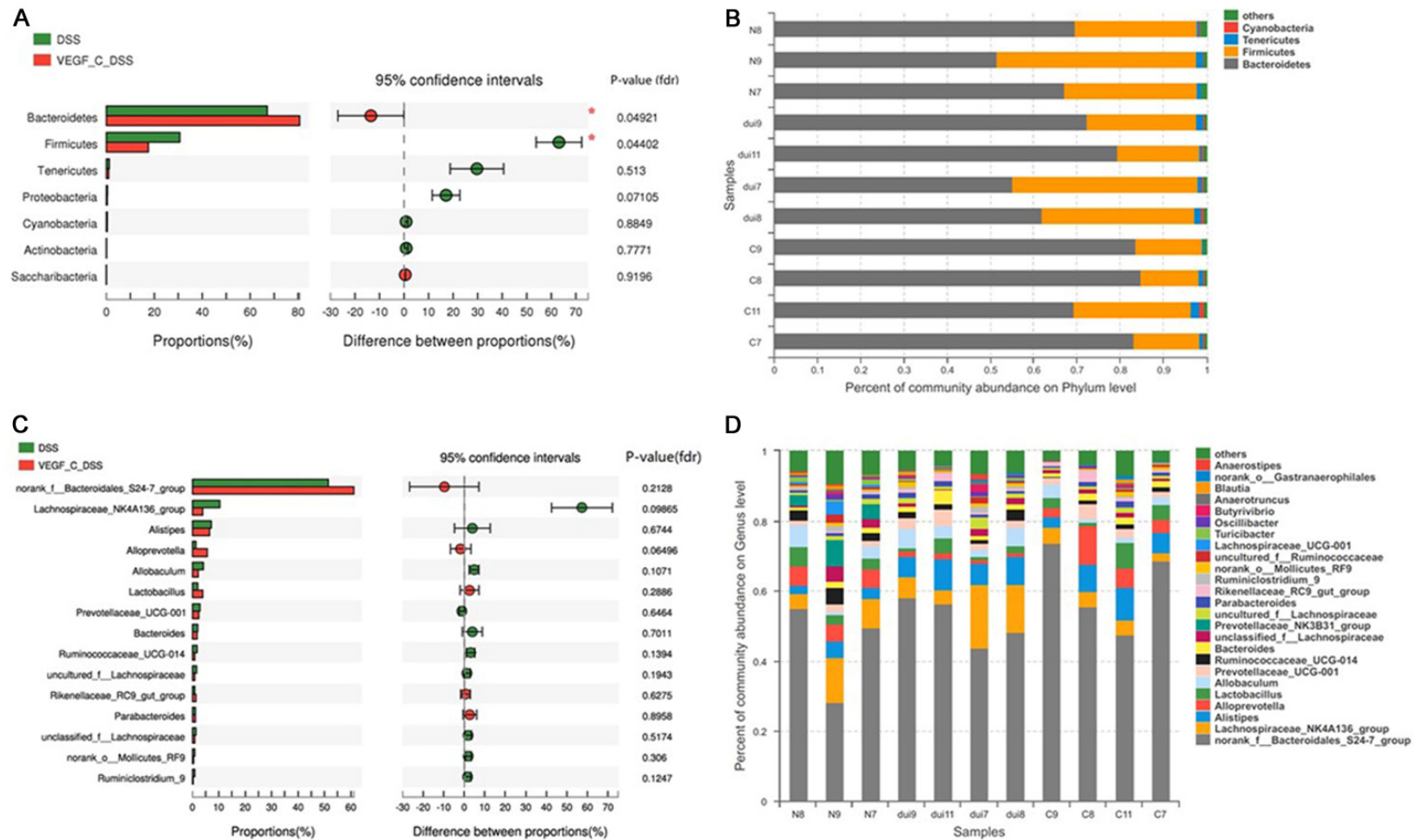


Figure 8. Influence of VEGF-C treatment on the microbiota at the phylum and genus levels in DSS-induced CC mice. A, B. After VEGF-C treatment, the proportion of Bacteroidetes significantly increased, but that of Firmicutes decreased when compared with DSS group ($P=0.049$ and 0.044 , respectively) at the phylum level. C, D. No significant difference were observed in these bacteria between Ad-VEGF-C group and DSS group at genus level ($P>0.05$).

VEGF-C mediated lymphatic drainage enhancement reduces intestinal inflammation

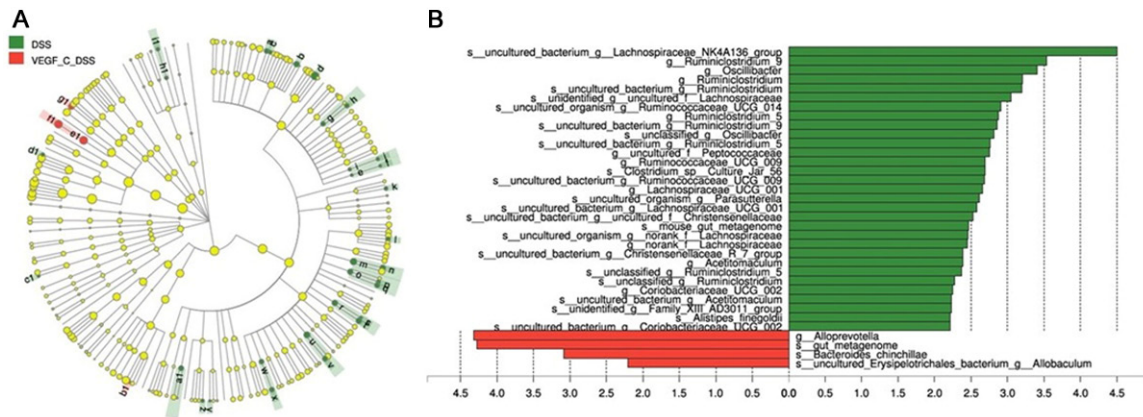


Figure 9. Cladograms indicating the polygenetic distribution of bacterial lineages associated with the different groups. Indicators between inner and outer mangrove sediments with LDA score larger than 2.5. LEfSe provided the features that are differential bacterial taxa ranking according to the effect size. Thirty-one taxa with significant difference were found in DSS group, and four taxa showed significant abundance in AD-VEGF-C group. Ad-VEGF-C group had higher abundance in four taxa as compared to DSS group. The percentage of *Alloprevotella* at the genus level and gut metagenome, *Bacteroides chinchilla* and uncultured *Erysipelotrichales_bacterium* at the species level changed significantly.

decreased significantly after AD-VEGF-C treatment as compared to DSS group (Figure 10D-F, $P=0.011$).

Discussion

IAL has been found to play a crucial role in the pathogenesis of inflammation. Stimulation of VEGF-C can improve chronic intestinal inflammation by increasing lymphangiogenesis, enlarging lymphatic vessels and enhancing lymphatic function [3]. In this study, we confirmed that Ad-VEGF-C treatment significantly improved CC by elevating lymphatic drainage. Furthermore, enhanced lymphatic drainage promoted Th9 cells (CD3⁺ T cells) and CD68⁺ macrophages removing from the colon, increased beneficial bacteria abundance and IL-17 level in the colon, but decreased colonic IL-9 level.

IAL may directly influence the degrees of mucosal edema and inflammation [18], however, its function is still poorly understood. Inflammatory cells and cytokines have a crucial role in the intestinal inflammation. Our results showed that the numbers of CD3⁺CD4⁺ T cells (Th 9 cells) and CD68⁺ macrophages decreased in VEGF-C treated CC mice as compared to mice in DSS group and VEGF-C treatment improved the lymphatic drainage function. Recently, several studies showed Th9 cells are involved in the pathogenesis of ulcerative colitis [3]. Although the Th1/Th2 paradigm has dominat-

ed the immunological mechanism of IBD for nearly two decades, recent advance indicates that many of the functions attributed to either Th1 or Th2 cells are increasingly becoming associated with the newly identified Th17 [17] and/or Th9 cells [18]. Until now, the role of IL-9 in UC has not yet been investigated. Th9 cells were labeled by transcriptional factor PU.1 in case of colitis in both humans and DSS treated mice. IHC revealed that most of PU.1 positive cells were CD3 positive lymphocytes in human UC specimens [4]. Therefore, CD3 positive cells were identified as Th9 cells in mouse colon in this study. IL-9 can promote the differentiation of Th9, and Th9 produces IL-9. Th9/IL-9 may impair intestinal barrier function *in vivo* [5, 19].

In our study, enhanced lymphatic drainage function after VEGF-C treatment promoted removal of Th9 cells from the colon, accompanied by the decreased colonic IL-9 level. The mouse colitis may be protected by improved intestinal mucosal barrier due to decreased IL-9 and Th9 cells. In mice, Th9 cells can produce IL-9 and IL-10. However, our results showed that low IL-9 level was accompanied by the elevated production of IL-10. Many factors influence the release of IL-10 in inflammatory environment. The decreased pro-inflammatory cytokines and increased anti-inflammatory cytokines finally relieve colitis.

Except for Th9/IL-9, other new types of effector CD4⁺ T cells such as Th17/IL-17 cells have been

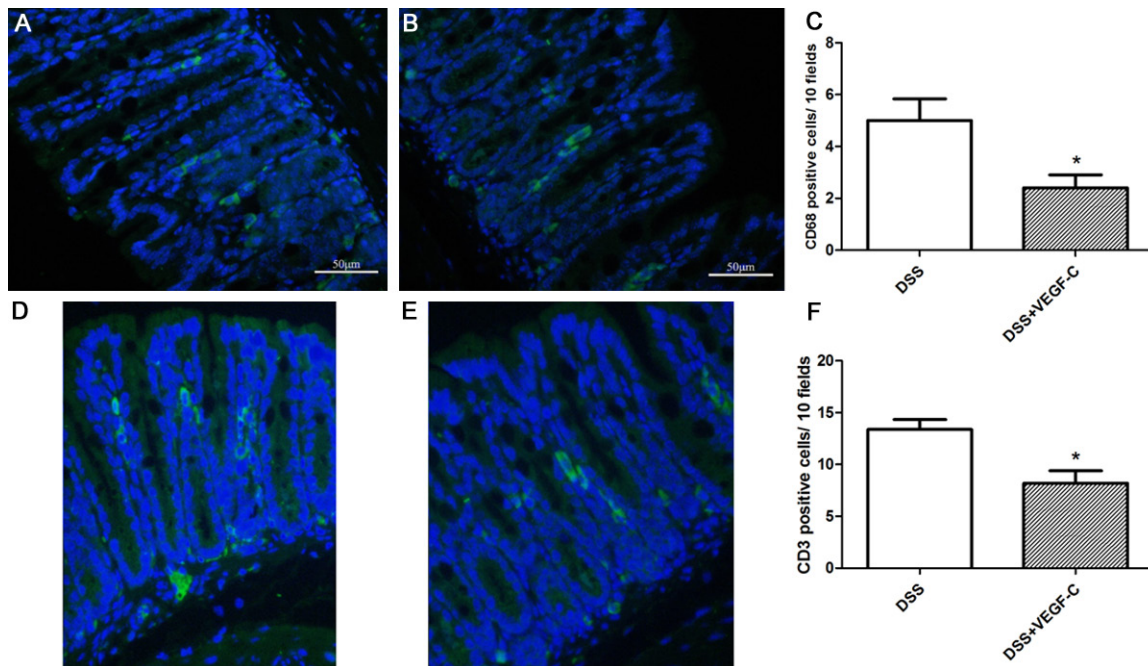


Figure 10. Macrophages and CD3⁺CD4⁺ T cells (Th9) inflammatory cells in the colon. The number of CD68⁺ macrophages (A-C) and CD3⁺CD4⁺ T cells (D-F) significantly reduced in VEGF-C-treated mice as compared to DSS group. Magnification: 200 \times , *t* test, **P*<0.05.

recently identified. Among investigated cytokines investigated, IL-9 mRNA levels best is closely related correlated with those of IL-6 and IL-17A [20, 21]. Th17 cells are a novel subset of T lymphocytes and have been found to be involved in the pathogenesis of chronic inflammation in UC via producing pro-inflammatory cytokines such as IL-17A. IL-17 is a pro-inflammatory cytokine playing varying roles in inflammation [22]. Although IL-17 was initially recognized as a pro-inflammatory cytokine, it can contribute to both induction and suppression of immune-mediated inflammation. In the CD45RBhi model, transfer of IL-17^{-/-} or IL-17RA^{-/-} CD45RBhi cells into RAG^{-/-} mice could deteriorate the disease as compared to mice treated with WT cells, demonstrating that IL-17 is protective [23]. However, in experimental models, results show an increase in the severity of granulomatous inflammation in mice correlates with high level of IL-17 and increased level of IFN- γ , demonstrating that IL-17 neutralization may improve the response to inflammation [24, 25]. Therefore, the functions of IL-17 vary among the different diseases, and the role of IL-17 in IBD remains unclear. IL-17 results in intestinal inflammation in some mouse studies but is pro-

tective in others [23-25]. In some studies of CD patients, the number of Th17 cells and the expression of Th17 cytokines increase in the intestinal tissues, which correlate with the disease activity [26, 27]. These results suggest that IL-17 play a dual role in disease activity and protection from mucosal damage [28]. Our results showed colon IL-17 increased after VEGF-C treatment and was protective by controlling inflammation. Some studies indicated the increased IL-17 may promote the proliferation of MDSCs [7] to suppress immune response [8, 9].

Clearance of intestinal bacteria is another function of lymphatics. However, few researches have explored the relationship between gut microbiota and lymphatic function of the intestine. Microbiota analysis revealed significant differences in the fecal microbial communities between CC mice with and without VEGF-C treatment. Although the α -diversity was significantly decreased in CC mice with VEGF-C treatment, VEGF-C treatment increased the abundance of phylum Bacteroidetes and reduced that of Firmicutes in CC mice. Our results suggest that to promote lymphatic drainage can

improve colitis by increasing beneficial gut microbiota. VEGF-C treatment decreased the relative abundance of Firmicutes at phylum level and its families Lachnospiraceae and Ruminococcaceae. Reduced abundance of the Firmicutes family members Ruminococcaeae and Lachnospiraceae is likely to affect the production of short chain fatty acids which are known to have anti-inflammatory activities and serve as fuel for colonic epithelial cells [10, 29]. Therefore, the change of gut microbiota in the VEGF-C-treatment mice group may exert a significant effect on the host health.

However, there are some limitations in our study. Although decreased IL-9 and increased IL-17 were found in CC mice, how IL-17 suppressed mucosal immune response and inhibited inflammation were still unclear, and the association of IL-9/IL-17A with IBD is needed to be further studied. The number of fecal samples for the detection of gut microbiota was small in this study. In the future, more fecal samples should be collected to analyze the change in gut microbiota after enhancing lymphatic drainage.

In conclusion, our study indicates VEGF-C treatment enhances the lymphatic drainage in DSS-induced CC, which then improves the gut microbiota. Meanwhile, the reduced Th9 cells after VEGF-C treatment may decrease IL-9 and increase IL-17, leading to the improvement of CC. Thus, VEGF-C may be a promising reagent for the treatment of CC.

Acknowledgements

This study was supported by a grant from the National Natural Science Foundation of China (#81200260 and #81670476).

Disclosure of conflict of interest

None.

Address correspondence to: Xiaolei Wang, Department of Gastroenterology, Shanghai Tenth People's Hospital, Tongji University, Shanghai 200072, China. E-mail: wangxiaolei@tongji.edu.cn

References

[1] Basson A, Trotter A, Rodriguez-Palacios A and Cominelli F. Mucosal interactions between genetics, diet, and microbiome in inflammatory bowel disease. *Front Immunol* 2016; 7: 290.

[2] Jurisic G, Sundberg JP and Detmar M. Blockade of VEGF receptor-3 aggravates inflammatory bowel disease and lymphatic vessel enlargement. *Inflamm Bowel Dis* 2013; 19: 1983-1989.

[3] D'Alessio S, Correale C, Tacconi C, Gandelli A, Pietrogrande G, Vetrano S, Genua M, Arena V, Spinelli A, Peyrin-Biroulet L, Fiocchi C and Danese S. VEGF-C-dependent stimulation of lymphatic function ameliorates experimental inflammatory bowel disease. *J Clin Invest* 2014; 124: 3863-3878.

[4] Yuan A, Yang H, Qi H, Cui J, Hua W, Li C, Pang Z, Zheng W and Cui G. IL-9 antibody injection suppresses the inflammation in colitis mice. *Biochem Biophys Res Commun* 2015; 468: 921-926.

[5] Weigmann B and Neurath MF. Th9 cells in inflammatory bowel diseases. *Semin Immunopathol* 2017; 39: 89-95.

[6] Cua DJ and Tato CM. Innate IL-17-producing cells: the sentinels of the immune system. *Nat Rev Immunol* 2010; 10: 479-489.

[7] Chen X, Churchill MJ, Nagar KK, Tailor YH, Chu T, Rush BS, Jiang Z, Wang EB, Renz BW, Wang H, Fung MC, Worthley DL, Mukherjee S and Wang TC. IL-17 producing mast cells promote the expansion of myeloid-derived suppressor cells in a mouse allergy model of colorectal cancer. *Oncotarget* 2015; 6: 32966-32979.

[8] Qin H, Lerman B, Sakamaki I, Wei G, Cha SC, Rao SS, Qian J, Hailemichael Y, Nurieva R, Dwyer KC, Roth J, Yi Q, Overwijk WW and Kwak LW. Generation of a new therapeutic peptide that depletes myeloid-derived suppressor cells in tumor-bearing mice. *Nat Med* 2014; 20: 676-681.

[9] Wesolowski R, Markowitz J and Carson WE 3rd. Myeloid derived suppressor cells - a new therapeutic target in the treatment of cancer. *J Immunother Cancer* 2013; 1: 10.

[10] Macfarlane S and Macfarlane GT. Regulation of short-chain fatty acid production. *Proc Nutr Soc* 2003; 62: 67-72.

[11] Cooper HS, Murthy SN, Shah RS and Sedergran DJ. Clinicopathologic study of dextran sulfate sodium experimental murine colitis. *Lab Invest* 1993; 69: 238-249.

[12] Nalleweg N, Chiriac MT, Podstawa E, Lehmann C, Rau TT, Atreya R, Krauss E, Hundorfean G, Fichtner-Feigl S, Hartmann A, Becker C and Mudter J. IL-9 and its receptor are predominantly involved in the pathogenesis of UC. *Gut* 2015; 64: 743-755.

[13] Amato KR, Yeoman CJ, Kent A, Righini N, Carbonero F, Estrada A, Gaskins HR, Stumpf RM, Yildirim S, Torralba M, Gillis M, Wilson BA, Nelson KE, White BA and Leigh SR. Habitat degradation impacts black howler monkey (*Alouatta pigra*) gastrointestinal microbiomes. *ISME J* 2013; 7: 1344-1353.

VEGF-C mediated lymphatic drainage enhancement reduces intestinal inflammation

- [14] Huggenberger R, Siddiqui SS, Brander D, Ullmann S, Zimmermann K, Antsiferova M, Werner S, Alitalo K and Detmar M. An important role of lymphatic vessel activation in limiting acute inflammation. *Blood* 2011; 117: 4667-4678.
- [15] Lozupone C and Knight R. UniFrac: a new phylogenetic method for comparing microbial communities. *Appl Environ Microbiol* 2005; 71: 8228-8235.
- [16] Segata N, Izard J, Waldron L, Gevers D, Miropolsky L, Garrett WS and Huttenhower C. Metagenomic biomarker discovery and explanation. *Genome Biol* 2011; 12: R60.
- [17] Korn T, Bettelli E, Oukka M and Kuchroo VK. IL-17 and Th17 Cells. *Annu Rev Immunol* 2009; 27: 485-517.
- [18] Kaplan MH. Th9 cells: differentiation and disease. *Immunol Rev* 2013; 252: 104-115.
- [19] Fallon PG, Richardson EJ, McKenzie GJ and McKenzie AN. Schistosome infection of transgenic mice defines distinct and contrasting pathogenic roles for IL-4 and IL-13: IL-13 is a profibrotic agent. *J Immunol* 2000; 164: 2585-2591.
- [20] Mudter J, Amoussina L, Schenk M, Yu J, Brustle A, Weigmann B, Atreya R, Wirtz S, Becker C, Hoffman A, Atreya I, Biesterfeld S, Galle PR, Lehr HA, Rose-John S, Mueller C, Lohoff M and Neurath MF. The transcription factor IFN regulatory factor-4 controls experimental colitis in mice via T cell-derived IL-6. *J Clin Invest* 2008; 118: 2415-2426.
- [21] Mudter J, Yu J, Zufferey C, Brustle A, Wirtz S, Weigmann B, Hoffman A, Schenk M, Galle PR, Lehr HA, Mueller C, Lohoff M and Neurath MF. IRF4 regulates IL-17A promoter activity and controls ROR γ -dependent Th17 colitis in vivo. *Inflamm Bowel Dis* 2011; 17: 1343-1358.
- [22] O'Connor W Jr, Kamanaka M, Booth CJ, Town T, Nakae S, Iwakura Y, Kolls JK and Flavell RA. A protective function for interleukin 17A in T cell-mediated intestinal inflammation. *Nat Immunol* 2009; 10: 603-609.
- [23] Smith PM, Shainheit MG, Bazzone LE, Rutitzky LI, Poltorak A and Stadecker MJ. Genetic control of severe egg-induced immunopathology and IL-17 production in murine schistosomiasis. *J Immunol* 2009; 183: 3317-3323.
- [24] Jiang W, Su J, Zhang X, Cheng X, Zhou J, Shi R and Zhang H. Elevated levels of Th17 cells and Th17-related cytokines are associated with disease activity in patients with inflammatory bowel disease. *Inflamm Res* 2014; 63: 943-950.
- [25] Yen D, Cheung J, Scheerens H, Poulet F, McClanahan T, McKenzie B, Kleinschek MA, Owyang A, Mattson J, Blumenschein W, Murphy E, Sathe M, Cua DJ, Kastelein RA and Rennick D. IL-23 is essential for T cell-mediated colitis and promotes inflammation via IL-17 and IL-6. *J Clin Invest* 2006; 116: 1310-1316.
- [26] Beringer A, Noack M and Miossec P. IL-17 in Chronic Inflammation: From discovery to targeting. *Trends Mol Med* 2016; 22: 230-241.
- [27] Sahin A, Calhan T, Cengiz M, Kahraman R, Aydin K, Ozdil K, Korachi M and Sokmen HM. Serum interleukin 17 levels in patients with Crohn's disease: real life data. *Dis Markers* 2014; 2014: 690853.
- [28] Hamour S, Gan PY, Pepper R, Florez Barros F, Wang HH, O'Sullivan K, Iwakura Y, Cook T, Pusey C, Holdsworth S and Salama A. Local IL-17 production exerts a protective role in murine experimental glomerulonephritis. *PLoS One* 2015; 10: e0136238.
- [29] Maslowski KM, Vieira AT, Ng A, Kranich J, Sierro F, Yu D, Schilter HC, Rolph MS, Mackay F, Artis D, Xavier RJ, Teixeira MM and Mackay CR. Regulation of inflammatory responses by gut microbiota and chemoattractant receptor GPR43. *Nature* 2009; 461: 1282-1286.